HHS Public Access

Author manuscript

Nat Chem Biol. Author manuscript; available in PMC 2011 February 01.

Published in final edited form as:

Nat Chem Biol. 2010 August ; 6(8): 602–609. doi:10.1038/nchembio.402.

Iron Traffics in Circulation Bound to a Siderocalin (Ngal)-Catechol Complex

Guanhu Bao[*,1], **Matthew Clifton**[*,2], **Trisha M. Hoette**[3], **Kiyoshi Mori**[4], **Shi-Xian Deng**[1], **Andong Qiu**[1], **Melanie Viltard**[1], **David Williams**[1], **Neal Paragas**[1], **Thomas Leete**[1], **Ritwij Kulkarni**[1], **Xiangpo Li**[1], **Belinda Lee**[1], **Avtandil Kalandadze**[1], **Adam J. Ratner**[1], **Juan Carlos Pizarro**[2], **Kai M. Schmidt-Ott**[5], **Donald W. Landry**[1], **Kenneth N. Raymond**[3], **Roland K. Strong**[#,2], and **Jonathan Barasch**[#,1]

[1]College of Physicians and Surgeons of Columbia University, New York

[2]Fred Hutchinson Cancer Research Center, Seattle

[3]University of California and the Lawrence Berkeley National Laboratory, Berkeley, California

[4]Kyoto University Graduate School of Medicine, Kyoto, Japan

[5]Max Delbruck Center for Molecular Medicine, Berlin, Germany

Abstract

The lipocalins are secreted proteins that bind small organic molecules. Scn-Ngal [known as Neutrophil Gelatinase Associated Lipocalin, Siderocalin, Lipocalin 2] sequesters bacterial iron chelators, called siderophores, and consequently blocks bacterial growth. However, Scn-Ngal is also prominently expressed in aseptic diseases, implying that it binds additional ligands and serves additional functions. Using chemical screens, crystallography, and fluorescence methods, we report that Scn-Ngal binds iron together with a small metabolic product called catechol. The formation of the complex blocked the reactivity of iron and permitted its transport once introduced into circulation *in vivo*. Scn-Ngal then recycled its iron in endosomes by a pH sensitive mechanism. Since catechols derive from bacterial and mammalian metabolism of dietary compounds, the Scn-Ngal:catechol:iron complex represents an unforeseen microbial-host interaction, which mimics Scn-Ngal:siderophore interactions, but instead traffics iron in aseptic

[#]**Corresponding Authors:** Roland K. Strong PhD, Division of Basic Sciences, Fred Hutchinson Cancer Center, 1100 Fairview Avenue North, Mailstop A3-025, Seattle, Washington 98109-1024, T: 206-667-5587, rstrong@fhcrc.org, Jonathan Barasch MD PhD, Department of Medicine, P&S 10-501, Columbia University, 630 West 168th St, New York, N.Y. 10032, T:212-305-1890, F: 212-305-3475, jmb4@columbia.edu.

[*]Equal Contribution

AUTHORS CONTRIBUTIONS:

G.B. identified siderophores, studied the complex in different models, and performed catechol chemistry. K.M., A.K.. B.L. initiated these studies. M.C. and R.K.S. identified the structure of Scn-Ngal and the critical sites of molecular recognition; T.M.H., X.L., S.D., D.W.L., A.J.R., J.C.P. and K.N.R. studied catechol and catechol:iron chemistry, binding affinity and pH sensitivity; N.P., A.Q., T.L., K.M.S and M.V. designed and performed cell biology experiments; D.W. performed radioautography, J.B. designed and analyzed experiments and, with contributions from all authors, wrote the paper. There are no conflicts of interests

Additional information

Supplementary information and chemical compound information is available online at http://www.nature.com/naturechemicalbiology/.

tissues. These results identify an endogenous siderophore, which may link the disparate roles of Scn-Ngal in different diseases.

The transport of iron among cells poses a significant problem because free ferric iron is insoluble ($< 10^{-18}$ M) in aerobic solutions at physiologic pH1. The solubilization of iron is also problematic because, even when it is bound to some chelators, iron remains capable of catalyzing reactions that produce toxic oxygen species2. Specialized mechanisms are consequently required to solubilize iron while inhibiting its chemical reactivity. These specialized mechanisms are found in proteins which utilize conserved motifs to directly bind iron (transferrin and ferritin) or in proteins with embedded cofactors such as sulfides3 or heme groups which chelate iron (IRP1, hemoglobin). While extracellular iron transport is largely mediated by transferrin operating in series with a few major-facilitator conductances, mice carrying deletions of these genes displayed surprisingly limited phenotypes4,5,6. Consequently additional, unknown pathways of iron transport are likely to function in parallel with the known transport proteins. We recently found that a member of the lipocalin superfamily acted as an iron carrier when binding a novel cofactor.

The lipocalins transport small organic ligands within a cavity (“calyx”) formed by a beta-barrel motif7. In the case of Scn-Ngal, the ligands include the bacterial siderophore enterochelin (Ent) from Gram-negative bacteria, bacillibactin from Gram-positive bacteria and carboxymycobactins from mycobacteria8,9. When these siderophores are bound to Scn-Ngal, iron transfer to bacteria is prevented and growth arrest is achieved8,9. Conversely, Scn-Ngal genetically deleted mice displayed excess growth of selected bacterial strains10,11. Consequently, Scn-Ngal demonstrates a novel mechanism of iron sequestration by a mammalian protein, reflecting mechanisms that are specific to particular types of infections.

Scn-Ngal is expressed at low levels *in vivo*, but a number of “damage” stimuli raise its concentration by orders of magnitude. These include bacterial ligands, but additionally, non-bacterial stimuli such as ischemia, antibiotics and cytotoxic agents which induce a 1000 fold increase in Scn-Ngal message and a 10–500 fold increase in Scn-Ngal in serum and urine10,12,13. Thereafter, Scn-Ngal traffics in the circulatory and urinary systems and is subsequently captured by one or more plasma membrane receptors including 24p3R14 and megalin12, suggesting that it delivers a ligand, both in the presence (bacterial siderophores) and in the nominal absence of bacterial infections (unknown ligands). While bacterial siderophores are not synthesized by mammalian cells, they are composites of well known functional groups such as hydroxybenzoates and hydroxybenzenes which are found in a variety of compounds in mammalian serum and urine15, suggesting that Scn-Ngal may bind these ligands. However, no additional Scn-Ngal ligands have been identified in mice or humans and most prior studies have relied on bacterially-expressed, recombinant Scn-Ngal, which already contains enterochelin.

Given that Scn-Ngal is abundant throughout the urinary system12,13, we chose mouse and human aseptic urine as a source of novel Scn-Ngal ligands. We developed assays to identify ligands which bind iron and Scn-Ngal. We found that a subset of catechols chelate iron and bind the Scn-Ngal calyx with subnanomolar affinity. The complexes could form *in vivo* and

deliver iron to cells through endosomes. We elucidated the mechanisms of iron association and dissociation from Scn-Ngal by structural analyses using x-ray crystallography and fluorescence quenching measurements, which revealed novel mechanisms of iron capture and iron release.

Results

Identification of the Scn-Ngal:Catechol:Iron Complex

Using paper chromatography, we found that protein-free filtrates (< 3 KDa) of urine were able to chelate iron (Supplementary Fig. 1). We then found that a component of the low molecular weight urine could associate with both Scn-Ngal and iron12 (Supplementary Fig. 2) even after this mixture underwent extensive buffer exchanges by different methods (Supplementary Figs. 3 and 4). In contrast, without the addition of urine, Scn-Ngal did not retain iron.

The activity of the urine filtrates (<3 KDa) was partially extractable with ethylacetate, demonstrating that it included organic molecules (Supplementary Fig. 2). Subsequently, a screen of urinary organic compounds15 identified 18 that mobilized iron on a paper chromatogram which we developed in water (Supplementary Fig. 5a and Supplementary Dataset 1). To determine whether these same compounds interacted with both Scn-Ngal and iron, we incubated Scn-Ngal (10 μM), urinary compounds (0.5–100 μM) and iron (1 μM ^{55}Fe +cold $FeCl_3$ 9 μM) and then washed these mixtures repetitively on a 10KDa cutoff filter (n = 4–7 independent experiments; Supplementary Fig. 5b). Among these active compounds, catechol, 3-methylcatechol, 4-methylcatechol and pyrogallol demonstrated saturable iron retention, but even compounds with more limited activity were structurally related. Hence, a screen of urinary compounds revealed a group of active molecules containing the catechol functional group. The interaction of these compounds with iron was specific in that iron binding activity was lost upon *O*-methylation or *O*-sulfonation of the hydroxyl groups (Supplementary Dataset 1). These findings were reminiscent of the interaction of Scn-Ngal with enterobacterial siderophores which, while structurally diverse, also contain catechol groups which chelate iron8,9. Indeed, Ent blocked the association of urinary catechols with Scn-Ngal (Supplementary Fig. 5c; n = 4–5 independent assays; $P<0.05–P<10^{-5}$) suggesting a critical role of catechol in binding to Scn-Ngal.

Cationic amino acids within the Scn-Ngal calyx recognize the catechol groups of Ent by interacting with their aromatic electron density and forming cation-π bonds16. To determine whether Scn-Ngal recognizes endogenous catechols by a similar type of interaction, we evaluated a mutant form of Scn-Ngal. Lysines K125 and K134 interact with the catechol groups of Ent8,9, and when both of these residues were mutated to alanine, Scn-Ngal became ineffective in the capture of both Ent:Fe and catechol:Fe (Supplementary Fig. 5d, n = 3–4, independent experiments; $P<0.005–10^{-5}$). To further analyze the interaction of cationic residues and catechol, we calculated the component of binding attributable to cation-π bonds8,9. The quadrupole moment of each catechol, as well as its corresponding quinone oxidation product was established (Supplementary Table 1). Then the cation (Na^+)-binding ability of the aromatic unit was calculated. These data indicated that, similar to Ent, simple catechols (catechol > 3-methylcatechol > pyrogallol) should have high affinity for

Scn-Ngal based on optimized cation- π interactions when bound in the calyx, but the quinone forms would be inactive. Together these data suggest that catechols and Ent share the same docking site within the Scn-Ngal calyx.

The association of catechol:iron complexes and Scn-Ngal was examined next. Remarkably, while catechol itself bound with poor affinity (K_d = 0.20±0.06 μM), we detected nanomolar interactions of catechol and Scn-Ngal in the presence of iron ^{III} (a 100 fold increase in binding affinity). Binding was best described by two dissociation constants (K_{d1} = 2.1±0.5 nM; K_{d2} = 0.4±0.2 nM; Fig. 1), suggesting a stepwise addition of ligands. Given the predicted pH sensitivity of the catechol:iron complexes, a di-catechol:iron ($Fe^{III}L_2$) complex was probably recruited first to the calyx at pH7.4 followed by a single additional catechol to generate an optimized hexadentate coordination of iron ($Fe^{III}L_3$) (see Fig. 2).17 In fact, a visible spectral from blue ($Fe^{III}L_2$: λ_{max} = 575 nm) to red ($Fe^{III}L_3$: λ_{max} = 498nm) resulted when catechol and iron^{III} were incubated with Scn-Ngal (Fig. 2), producing a spectrum that was identical to the *tris*-catecholate Ent:Fe^{III}. The spectral shift occurred because strong-field catechol ligands ($Fe^{III}L_n$ + L=>$Fe^{III}L_{n+1}$) destabilized iron t_{2g} orbitals, increasing the energy-gap between the ligand and metal orbitals that are involved in charge transfer and accounting for the spectral shift to higher energy18,19. The red shift was stable for at least 48hrs at room temperature. Hence the formation of a *tris*-catecholate coordination structure ($Fe^{III}L_3$), which maximizes both cationic-π interactions ($Fe^{III}L_3$ contains three catechol groups) as well as Coulombic interactions ($Fe^{III}L_3$ is trianionic) within the Scn-Ngal calyx was likely the mechanism by which the addition of iron^{III} increased the affinity for catechols. In contrast, little, if any $Fe^{II}L_2$ or $Fe^{II}L_3$ formed in solution or within the Scn-Ngal calyx, respectively, since appropriate spectral changes were limited, and quenched with the addition of ascorbate which limited Fe^{II} oxidation (Supplementary Fig. 6). Hence, in the presence of Fe^{III}, Scn-Ngal generates a high affinity catechol:iron complex, by using cationic-π and electrostatic interactions to recruit its components.

Structural Studies

To define the specific binding site for the catechols, Scn-Ngal and catechol:iron were co-crystallized using conditions established for the Scn-Ngal:Ent:iron complex (pH 4.5). Structures (d_{min} = 2.3Å) were determined by direct phasing from a prior structure (PDB accession code 1L6M) and refined to acceptable statistics (Supplementary Table 2). While diffraction data were collected from a number of complexes, difference Fourier syntheses showed clear, unambiguous ligand density only for catechol:iron and 4-methylcatechol:iron. The binding of 4-methylcatechol was observed in spite of its low affinity for Scn-Ngal (Fig. 1a, b) reflecting the high concentration of ligand in the crystallization conditions. None of these ligands significantly affected the overall structure of Scn-Ngal when compared with previous structures (PDB accession codes 1DFV, 1QQS, 1L6M, 1X71, 1X89, 1X8U)8,9,20. For example, pairwise superposition RMSDs between the molecules of the Scn-Ngal:Ent:Fe complex (1L6M) are X1, Y1, and Z1 for catechol:Fe; and X2, Y2, and Z2 for the 4-methylcatechol:Fe complex (calculated on all common C-alphas in the asymmetric unit). Molecule B showed higher disorder, reflected in poorer quality electron densities and higher B-factors (Supplementary Table 2), accounting for the greater disparity among these molecules. Structural conservation extended to residues making direct contact with ligands

in the calyx except for residues W79 and R81 which adopted alternate rotamers from those seen in the Ent:iron complex.

A single catechol or 4-methylcatechol occupied pocket #18,20 between the side-chains of lysines K125 and K134 (Fig. 3). 4-methylcatechol was rotated so that the hydroxyl groups faced down into the calyx and the ligand was shifted upwards (~1Å) out of the calyx; this shift accommodated the methyl substitution and relieved steric clashes in pocket #1 (Fig. 3, Supplementary Fig. 7). With the exception of the rotation of the catechol around an axis perpendicular to the rings, they superimposed with the phenyl groups of Ent and Carboxymycobactin in corresponding Scn-Ngal complexes (Supplementary Fig. 8).

Both catechol and 4-methylcatechol were found to coordinate iron, but as a result of the crystallization at pH 4.5 (see below), which limits binding (Supplementary Fig. 6) or alternatively as a result of the oxidation of catechol to semiquinone, iron was coordinated by one catechol hydroxyl group (Fig. 3), the second facing out of the calyx, resulting in partial occupancy of iron binding sites. The lack of full hexacoordination of iron also created a net positive charge, which was compensated by the variable binding of chloride atoms in the calyx (Supplementary Fig. 9). These data show that pocket #1 determines ligand specificity by contributing the highest affinity for polarized aryl groups.

Traffic of Scn-Ngal:Catechol:Iron

To test whether Scn-Ngal binds and transports catechol *in vivo*, we introduced Scn-Ngal and catechol:Fe^{III} separately into C57BL/6 mice and harvested the serum 5 minutes later. Scn-Ngal and catechol formed a complex in circulation that was detectable when we fractionated the sera by gel filtration (Fig. 4a). Over time, the complex was captured by a variety of organs including the kidney, the lung and liver, whereas unbound catechol in comparison was rapidly cleared (Fig. 4b). The lung (P = 0.013 at 20 min), the liver (P = 0.027 and P = 0.024 at 20 and 180 min, respectively) and the kidney (P = 0.0036 and P = 0.0217 at 20 and 180 min) contained significantly more Scn-Ngal:catechol:Fe complex than free catechol (n = 4 independent experiments), particularly the kidney which retaining most of the complex (liver vs. kidney; P = 0.044 at 180 min). Consistently, the Scn-Ngal:catechol complex delivered iron to the kidney (Fig. 4c). The distribution of iron was not likely the result of an exchange of iron with the citrate pool, because while Scn-Ngal:catechol:Fe targeted the kidney, citrate:Fe which is not bound by Scn-Ngal (Supplementary Dataset 1) preferentially targeted the liver (in liver: citrate:Fe>Scn-Ngal:catechol:Fe P = 0.0068; in kidney: Scn-Ngal:catechol:Fe>citrate:Fe P = 0.027; n = 5–7 independent experiments at 180 min). The targeting of iron was also not likely the result of an exchange of iron with the transferrin pool, because transferrin:iron did not target the kidney (in kidney: Scn-Ngal:catechol:Fe > transferrin:Fe P = 0.0068, n = 5–7 independent experiments at 180 min) but rather accumulated in the bone marrow. Radioautography demonstrated that Scn-Ngal:catechol:Fe delivered iron to the proximal tubule of the kidney (silver grains in Fig. 4d) whereas citrate:Fe was not found in the kidney (Fig. 4e). Delivery of iron to the kidney most likely involved glomerular filtration of Scn-Ngal:catechol:Fe12 followed by endocytosis at the apical membrane of the proximal tubule via the megalin receptor21 since Scn-Ngal was found in the urine of megalin knock-out mice12, 22 (Supplementary Fig. 10). These data

show that Scn-Ngal can transport catechol:iron in the circulation, eventually disposing of these ligands in the kidney.

Effective chelation of iron by a carrier should not only result in its transport, but also in limiting its reactivity. Catechols activate the Fenton reaction2,23 by reducing iron (Fe^{III}=>Fe^{II}) and thereby accelerating hydroxyl-radical formation. We confirmed these data by detecting phenanthroline reactive Fe^{II} after incubating Fe^{III} with catechol, pyrogallol, 3-methylcatechol or 4-methylcatechol. However, the addition of stoichiometric quantities of Scn-Ngal (Scn-Ngal:catechol 1:3, respectively) inhibited the reaction (e.g. catechol+$FeCl_3$ ± Scn-Ngal: P< 10^{-4}; pyrogallol+$FeCl_3$±Scn-Ngal: P< 0.005, two-tailed *t*-test, n=4; Supplementary Fig. 11a). Likewise, while catechol:Fe induced the conversion of 3-(*p*-hydroxyphenyl) fluorescein (HPF) to fluorescein in the presence of H_2O_2, the addition of Scn-Ngal blocked the reaction (e.g. HPF+catechol+$FeCl_3$ ± Scn-Ngal: P< 10^{-5}, n=3; Supplementary Fig. 11b). In contrast, the protein did not affect the fluorescein control molecule24. *O*-sulfonation or *O*-methylation of catechol hydroxyl groups prevented the reduction of iron as well as the generation of radicals (HPF+catechol+$FeCl_3$ vs HPF +catechol-sulfonate+$FeCl_3$ $P<10^{-5}$, two-tailed *t*-test, n=3), demonstrating that the hydroxyl groups were required for iron mediated reactivity. These data demonstrate that by sequestering catechol:iron complexes, Scn-Ngal maintained $iron^{III}$ oxidation, and thereby limited iron reactivity in Fenton type reactions.

To transport iron into cells, there has to be a mechanism for iron release from the calyx. Intracellular delivery of iron by transferrin is known to require passage through acidified endosomes, whereupon iron is released. We tested whether a similar mechanism existed for the Scn-Ngal:catechol:iron complexes. We found that while these complexes were stable at neutral pH, acidification below pH 7.0 progressively reversed ligand-dependent fluorescence quenching of Scn-Ngal (n =3 independent preparations of Scn-Ngal, Fig. 5a). Catechol and 3-methylcatechol complexes dissociated by pH 6.0, while pyrogallol and 2,3DHBA complexes resisted acidification until below pH 4. Consistently, acidification also released iron (Fig. 5b), the catechol complex being more sensitive to acidification than the pyrogallol or Ent complexes of Scn-Ngal (respectively, P = 0.0017; P =0.00012 at pH 5.5, n=4, two tailed *t*-test). Acid dependent dissociation was likely due to protonation of the catechol hydroxyls or amino acids within the calyx, rather than the unfolding of Scn-Ngal19. These findings explain the presence of a single catechol in the pH 4.5 crystal, implying that our crystal structures represented the final stages of pH-mediated ligand release.

To test the relevance of the pH sensitivity of the Scn-Ngal:catechol:iron complex in a biologically relevant assay, we added the radiolabeled complex to cells, and demonstrated iron donation. This process was blocked at 4°C (37°C vs 4°C, LLCPK cells $^{**}P < 0.005$ or stromal cells $^{***}P < 10^{-4}$) and when the vacuolar H^+ATPase of endocytic vesicles was inhibited with bafilomycin, suggesting that iron donation required endosomal trafficking of the complex (n = 5, Fig. 5c). Uptake occurred in both a stromal cell line25 and in a proximal tubule epithelial cell line from the kidney (LLCPK cells, Supplementary Fig. 12). Hence, unlike Ent:iron whose dissociation required more extreme acidification, the binding properties of catechol:iron and related molecules ideally matched the cellular requirements for the transport and delivery of iron to cells.

To determine whether Scn-Ngal:catechol:Fe might deliver sufficient iron to regulate iron responsive genes, we utilized polarized LLCPK cells which, when grown on a fibronectin coated filter to confluence, captured Alexa-568-Scn-Ngal from the apical media (Supplementary Fig. 12a). A previously characterized iron responsive YFP probe26 was transfected into these cells and holo-transferrin+ferric ammonium citrate or the iron chelator deferoxamine were added to the apical media as positive and negative controls, respectively (Supplementary Fig. 12b–g). The Scn-Ngal:catechol:Fe complex activated the iron dependent YFP probe (100μg/ml, P =0.0011, 500μg/ml P =0.0016, n=3, compared to DMEM alone). This was detected spectrophotometrically in lysed cells, as well as by fluorescent microscopy. Taken together with the iron uptake experiments, these data indicate that Scn-Ngal can traffic and deliver iron to cells.

Source of Catechols

Catechols are abundant metabolites in mammals. They are derived from polyphenols such as quinic and shikimic acids (~50%;)27,28,29,30 and aromatic amino acids (~50%)28,30,31. We confirmed the existence of the latter pathway by incubating ^{3}H-tyrosine with dissociated lung or intestinal cells (but not with spleen, liver or heart cells; Supplementary Fig. 13) at 37°C overnight, which in turn generated ^{3}H-catechol, as demonstrated by HPLC with *0*-methylation studies. Other aromatic amino acids such as ^{3}H-phenylalanine and ^{3}H-tryptophan were not effective substrates for catechol (n = 3).

Catechols are excreted in large quantities in urine, as demonstrated by HPLC analysis of urine (Supplementary Fig. 14). Indeed, 80.56±8.8% of catechol and 56.4±6.7% of Scn-Ngal:catechol were cleared in the urine by 180 min after introducing these components, the difference reflecting Scn-Ngal:catechol uptake in kidney and other organs (P = 0.019). Subsequently, catechol are sulfonated32 to cyclic and mono-catechol sulfate (Supplementary Dataset 1) which blocks further interactions with iron, but 1–5% of the total27,28, or approximately 10 fold the peak levels of urinary Scn-Ngal (induced by kidney damage) remain non-sulfated. Non-sulfonated catechol was stable in solution (as monitored for 20 hrs by NMR; D_2O: 6.9 ppm, 2H; 6.7 ppm, 2H) and readily detected in the urine by ESI mass spectroscopy (109 m/z peak; negative mode). The peak was then further authenticated by methylation and detection of methylated products by TLC and mass spectroscopy (Supplementary Fig. 15). In sum, the catechols are abundant metabolic products in mammals that derive from components of food, in part by the metabolic actions of microorganisms.

Discussion

Structural analyses8,9 first suggested that Scn-Ngal may bind ligands other than bacterial siderophores. This is because the major Scn-Ngal ligand, Ent is composed of functional groups that are synthesized not only by bacteria, but also by mammalian cells, implying that ‘endogenous’ ligands may bind Scn-Ngal. Here we show that a family of common metabolites, called the catechols permitted high affinity binding, effective sequestration and the transport of iron to cells of the kidney by Scn-Ngal. The data are reminiscent of classical

reports which showed that low molecular weight iron chelators are synthesized by mammalian cells33.

The origin of mammalian catechols has not been fully explained. Dietary intake of plant quinic, shikimic27, and 3,4-dihydroxybenzoic acids28 may contribute since rats fed quinic acid, for example, excrete both free and conjugated catechol in the urine27. Likewise, plant hydroxybenzenes such as caffeic acid, chlorgenic acid, catechin, and epicatechin can undergo conversion into catechol29. The restriction of dietary plants consistently reduced the urinary catechols in half to 40 μM30 while increasing the 4-methylcatechol component implied that additional pathways contribute to the catechols such as the conversion of dietary protein to phenol and then to catechol by a NADPH dependent liver microsomal cytochrome P450 34 , 35 . Microorganisms28 are involved in these pathways since oral neomycin, which sterilizes the gut, reduces catechol excretion in half36 and we found that urine from mice fed antibiotics or raised in a gnotobiotic facility contained one-half of the siderophore activity as did conventional urine. Hence the catechols may join the list of 'co-metabolites' which derive from intestinal microbes but have function in metabolic reactions in the mammalian host37. In this light, the Ngal-Scn:catechol complex is an example of a bacterial-host interaction, and a second example, after Ent chelation, by which Ngal-Scn interacts with bacterial products, albeit in this case the products of endogenous microflora in the "non-infected" state.

Urinary catechols are highly abundant: catechol is present at 150 μM34,38 ,39 , 4-methylcatechol at 30 μM, and pyrogallol at 500 μM29,30 (free catechols are 1–5% of these totals). This means that when Scn-Ngal plasma levels rise 10–50010,12,13 fold (0.1μM) and iron is released from damaged tissues (such as the kidney affected by acute injury and glomerular diseases),40,41,42, Scn-Ngal (~0.1 μM) may be constitutively saturated by excess free catechol (~1 μM), especially given that the presence of iron enhances the affinity for the complex 100 fold. Hence, perhaps even as much as 400 mg (17 μmole) of Scn-Ngal12, ~1mg of iron and ~2mg catechol may undergo filtration by the glomerulus and recycling in the proximal tubule per day by a megalin (Supplementary Fig. 10) or 24p3R dependent endosomal pathway. These data emphasize the potential role of Scn-Ngal as a scavenger of catechol, which is known to mobilize Fe^{III} even from proteins17, and a scavenger of the catechol:iron complex, which is known to participate in Fenton reactions2,22. Ligation by the Ngal-Scn calyx conversely quenched iron reduction and hydroxyradical activation by catechol:iron. Additionally, since the donation of iron to microbes may be facilitated by different types of catechols such as 2,3-dihydroxybenzoic acid (Salmonella43 and Brucella) and catecholamines (E. coli 44 and Bordatella 45), the clearance of the Scn-Ngal:catechol:iron complex in the kidney might also serve a broad role in the defense against microorganisms, sharing this property with the clearance of Scn-Ngal:Ent:iron by the kidney12.

Since Scn-Ngal is induced in several human cancers and correlates with a poor prognosis46, a model has been proposed where *i*) receptor-mediated endocytosis of extracellular Scn-Ngal:iron complexes delivered iron to cells and prevented apoptosis or where *ii*) internalization of ligand free Scn-Ngal by cells lead to iron efflux resulting in apoptosis and cell death, mediated by the pro-apoptotic protein Bim14. The results presented here describe

the candidate endogenous siderophores necessary for supporting these proposed mechanisms.

In conclusion, we have identified a new family of iron binding cofactors. While cofactors such as heme and sulfide groups are well known in intracellular proteins, we describe a novel iron binding cofactor in an extracellular carrier protein that mimics in structure and molecular recognition a classical bacterial siderophore. The metabolic fate of iron released in tissue injury has been unknown, but here we show that a constitutively produced siderophore, catechol, complexed with a stress activated protein, Scn-Ngal, traffics and clears iron. This pathway may be quantitatively significant in renal proximal tubule epithelia, where iron is recycled, and perhaps in the urine as well where the Scn-Ngal:catechol:iron complexes are discarded.

Methods

Chemicals and Animal Samples

Compounds were obtained commercially (Supplementary Dataset 1). All solvents were HPLC grade from Fisher. Catechol-^{14}C (100 mCi/mmol) was from Sigma and L-[5-^{3}H]Tryptophan (32.0 Ci/mmol) , L-[4-^{3}H]Phenylalanine (27.0 Ci/mmol), and L-[3,5-^{3}H]Tyrosine (54.0 Ci/mmol) were from Amersham-GE Healthcare. $^{55}FeCl_3$ (45mCi/mg) was from PerkinElmer. Desferri-Enterochelin (Ent) and ferric Ent (Ent:Fe) were from EMC Microcollections, Germany. Ngal-Scn was expressed in BL-21 bacteria8,9. Blood, urine and tissues of mice and procedures were performed with approval of the Institutional Animal Care and Use Committee (IACUC) at Columbia University. CD1 Mouse urine was also obtained from the Bioreclamation Company, New York, before and after treatment with oral Vancomycin and Neomycin for 1 week. Human urine was pooled from healthy medical school students as well as from patients of Columbia University Medical Center, with approval of the Institutional Review Board.

Computational Methods

Computational studies were conducted at the Molecular Graphics and Computation Facility, College of Chemistry, University of California, Berkeley. To determine the quadrupole moments, Θ_{zz}, the aromatic structures were geometry optimized and characterized via frequency calculations at the RHF/6-311G** level of theory in the Gaussian 03 package47. To determine the aromatic-cation interaction energies the components were characterized via a frequency calculation at the MP2/6-311++G** level of theory and the aromatic-cation interaction energies corrected for basis set superposition error (BSSE) with the counterpoise method in the Gaussian 03 package. In the aromatic-cation calculations the sodium ion was fixed at a distance of 2.47 Åabove the centroid of the aromatic unit.

Crystallography

Recombinant C87S human Scn-Ngal was expressed and purified as previously described8,9. Protein (10 mg/ml) was mixed with 10 mM catechol or 4-methylcatechol and then with 5 mM $FeCl_3$, using extensive washes (YM-10, Millipore) with PNE (25 mM PIPES, 150 mM NaCl, and 1 mM EDTA). Co-crystals of ligand bound human Scn-Ngal were grown by

vapor diffusion at 18 °C over reservoirs of 1.0–1.4 M NH_4SO_4, 100 mM NaCl, 50 mM $LiSO_4$, 100 mM Na acetate (pH 4.5). Crystals typically grew in 5–10 days and were cryo-protected using the mother liquor plus 15% glycerol prior to flash cooling in $LiqN_2$. Diffraction data were collected using synchrotron radiation at the Advanced Light Source (Berkeley, CA) beamline 5.0.1 (wavelength 1.0λ) (Supplementary Methods). Relevant statistics are shown in Supplementary Table 1 and coordinates deposited in the Protein Data Bank: www.rcsb.org (Accession Codes: Catechol = 3FW4; 4-methylcatechol = 3FW5).

Binding Assays

(Supplementary Methods) We utilized fluorescence quenching to measure the affinity of the Scn-Ngal:catechol interaction. Excitation λ_{exc} = 281 nm (5 nm slit band pass) and emission λ_{em} = 340 nm (10 nm slit band pass) data were collected from 100 nM protein solutions (with 32μg/mL ubiquitin and 5% DMSO) exposed to ligands. To prepare FeL_3, catechol (12 mM, 25μL in DMSO) and ferric chloride (0.33eq.) were combined and then diluted to form the metal complex 18 μM FeL_2 (in iron) in aqueous buffer (pH 7.4; TBS) and 5% DMSO. Apo-catechol solutions were prepared analogously. The pH was adjusted with 0.1 M HCl incrementally until the fluorescence signal stopped changing, while fluorescence values were corrected for dilution. To monitor the stability of the complex over time, the sample was stored at 4 °C for 12 hrs. Data were analyzed by a nonlinear regression analysis using a one-site binding model (DYNAFIT)48. Control experiments were performed to ensure the stability of the protein at experimental conditions, including the dilution and the addition of DMSO and ubiquitin.

Scn-Ngal:Siderophore:Iron Traffic

(Supplementary Methods) Mouse embryonic kidney $FoxD1^+$ stromal cells25 (10^5 cells) and adult kidney proximal tubule LLCPK1 cells (10^5 cells, ATCC, CL101) were grown in DMEM (low glucose) with 10% FCS for 24 hrs, the FCS removed and complexes Scn-Ngal:^{14}C-catechol or Scn-Ngal:catechol:^{55}Fe, prepared as above, were added to the cells at 37 °C or 4 °C for 0–6 hrs. Bafilomycin (0.15 nmole) was tolerated by stromal cells for 3 hrs. Cells were then washed 3 times, briefly trypsinized, and then collected and measured by scintillation counting. To examine the capture of Scn-Ngal in different tissues, the Scn-Ngal complexes were introduced by an intraperitoneal route and tissues harvested 1–6 hrs later from C57BL/6 wild type, 8 week old male mice (Charles River) housed with food and water ad libitum. Tissues were diced and dissolved in 2% SDS, 0.1 N NaOH at 60 °C and counted. Each experiment was repeated 3–7 times using independent preparations of recombinant mouse Scn-Ngal and results expressed as means ± s.d. with independent two-tailed Student *t*-tests. For radioautography, the kidneys were fixed in 4% glutaraldehyde in phosphate buffer, post-fixed in 1% OsO_4 and embedded in Epon812. Sections (1 μm) were coated with Ilford K5D emulsion and developed with Microdol (Kodak) after a 2 month exposure.

Supplementary Material

Refer to Web version on PubMed Central for supplementary material.

ACKNOWLEDGMENTS

We thank Drs. Rebecca Abergel, Anna Zawadzka, Q. Al-Awqati for helpful discussion. We are grateful to the Gordon lab for gnotobiotic urines and EI Christensen and TE Willnow for megalin knockout urines. We salute the Medical School Classes of 2010 and 2013, College of Physicians and Surgeons for donating urine for this study. Supported by NIH grants AI117448 (KNR), AI59432 (RKS) and the Emerald Foundation, the March of Dimes and by NIH grants DK-55388 and DK-58872 (JB).

References

1. Theil EC, Goss DJ. Living with iron (and oxygen): questions and answers about iron homeostasis. Chem. Rev. 2009; 109:4568–4579. [PubMed: 19824701]
2. Iwahashi H, Morishita H, Ishii T, Sugata R, Kido R. Enhancement by catechols of hydroxyl-radical formation in the presence of ferric ions and hydrogen peroxide. J. Biochem. 1989; 105:429–434. [PubMed: 2543661]
3. Rouault TA, Tong WH. Iron-sulfur cluster biogenesis and human disease. Trends Genet. 2008; 24:398–407. [PubMed: 18606475]
4. Li JY, et al. Scara5 is a ferritin receptor mediating non-transferrin iron delivery. Dev. Cell. 2009; 16:35–46. [PubMed: 19154717]
5. Levy JE, Jin O, Fujiwara Y, Kuo F, Andrews NC. Transferrin receptor is necessary for development of erythrocytes and the nervous system. Nat. Genet. 1999; 21:396–399. [PubMed: 10192390]
6. Gunshin H, et al. Slc11a2 is required for intestinal iron absorption and erythropoiesis but dispensable in placenta and liver. J Clin. Invest. 2005; 115:1258–1266. [PubMed: 15849611]
7. Akerstrom B, Flower DR, Salier JP. Lipocalins: unity in diversity. Biochim. Biophys. Acta. 2000; 1482:1–8. [PubMed: 11058742]
8. Goetz DH, et al. The neutrophil lipocalin NGAL is a bacteriostatic agent that interferes with siderophore-mediated iron acquisition. Mol. Cell. 2002; 10:1033–1043. [PubMed: 12453412]
9. Holmes MA, Paulsene W, Jide X, Ratledge C, Strong RK. Siderocalin (Lcn 2) also binds carboxymycobactins, potentially defending against mycobacterial infections through iron sequestration. Structure. 2005; 13:29–41. [PubMed: 15642259]
10. Flo TH, et al. Lipocalin 2 mediates an innate immune response to bacterial infection by sequestrating iron. Nature. 2004; 432:917–921. [PubMed: 15531878]
11. Berger T, et al. Lipocalin 2-deficient mice exhibit increased sensitivity to Escherichia coli infection but not to ischemia-reperfusion injury. Proc. Natl. Acad. Sci. USA. 2006; 103:1834–1839. [PubMed: 16446425]
12. Mori K, et al. Endocytic delivery of lipocalin-siderophore-iron complex rescues the kidney from ischemia-reperfusion injury. J. Clin. Invest. 2005; 115:610–621. [PubMed: 15711640]
13. Mishra J, et al. Neutrophil gelatinase-associated lipocalin (NGAL) as a biomarker for acute renal injury after cardiac surgery. The Lancet. 2005; 365:1231–1238.
14. Devireddy LR, Gazin C, Zhu X, Green MR. A cell-surface receptor for lipocalin 24p3 selectively mediates apoptosis and iron uptake. Cell. 2005; 123:1293–1305. [PubMed: 16377569]
15. Wishart DS, et al. HMDB: the Human Metabolome Database. Nucleic Acids Res. 2007; 35:D521–D526. [PubMed: 17202168]
16. Hoette TM, et al. The role of electrostatics in siderophore recognition by the immunoprotein Siderocalin. J. Am. Chem. Soc. 2008; 130:17584–17592. [PubMed: 19053425]
17. Sánchez P, et al. Catechol releases iron (III) from ferritin by direct chelation without iron (II) production. Dalton Trans. 2005; 4:811–813. [PubMed: 15702194]
18. Karpishin RB, Gebhard MS, Solomon EI, Raymond KN. Spectroscopic studies of the electronic structure of iron(III) tris(catecholates). J. Am. Chem. Soc. 1991; 113:2977.
19. Abergel RJ, et al. The Siderocalin/Enterobactin interaction: A link between mammalian immunity and bacterial iron transport. J. Am. Chem. Soc. 2008; 130:11524–11534. [PubMed: 18680288]
20. Goetz DH, et al. Ligand preference inferred from the structure of neutrophil gelatinase associated lipocalin. Biochemistry. 2000; 39:1935–1941. [PubMed: 10684642]

21. Hvidberg V, et al. The endocytic receptor megalin binds the iron transporting neutrophil-gelatinase-associated lipocalin with high affinity and mediates its cellular uptake. FEBS Lett. 2005; 579:773–777. [PubMed: 15670845]
22. Leheste JR, et al. Megalin knockout mice as an animal model of low molecular weight proteinuria. Am. J. Pathol. 1999; 155:1361–1370. [PubMed: 10514418]
23. Rodríguez J, Parra C, Contreras FJ, Baeza J. Dihydroxybenzenes: driven Fenton reactions. Water Sci. Technol. 2001; 44:251–256. [PubMed: 11695467]
24. Setsukinai K, et al. Development of novel fluorescence probes that can reliably detect reactive oxygen species and distinguish specific species. J. Biol. Chem. 2003; 278:170–3175.
25. Levinson RS, et al. Foxd1-dependent signals control cellularity in the renal capsule, a structure required for normal renal development. Development. 2005; 132:529–539. [PubMed: 15634693]
26. Li JY, et al. Detection of intracellular iron by its regulatory effect. Am. J. Physiol. Cell Physiol. 2004; 287:C1547–C1559. [PubMed: 15282194]
27. Booth AN, Robbins DJ, Masri MS, DeEds F. Excretion of catechol after ingestion of quinic and shikimic acids. Nature. 1960; 187:691. [PubMed: 13802680]
28. Martin AK. The origin of urinary aromatic compounds excreted by ruminants. 3. The metabolism of phenolic compounds to simple phenols. Br. J. Nutr. 1982; 48:497–507. [PubMed: 7171537]
29. Lang R, Mueller C, Hofmann T. Development of a stable isotope dilution analysis with liquid chromatography-tandem mass spectrometry detection for the quantitative analysis of di- and trihydroxybenzenes in foods and model systems. J. Agric. Food Chem. 2006; 54:5755–5762. [PubMed: 16881674]
30. Carmella SG, La VEJ, Hecht SS. Quantitative analysis of catechol and 4-methylcatechol in human urine. Food Chem. Toxicol. 1982; 20:587–590. [PubMed: 6890513]
31. Bakke OM. Urinary simple phenols in rats fed purified and nonpurified diets. J. Nutr. 1969; 98:209–216. [PubMed: 5783302]
32. Rennick B, Quebbemann A. Site of excretion of catechol and catecholamines: renal metabolism of catechol. Am. J. Physiol. 1970; 218:1307–1312. [PubMed: 5438255]
33. Jones RL, Peterson CM, Grady RW, Cerami A. Low molecular weight iron-binding factor from mammalian tissue that potentiates bacterial growth. J. Exp. Med. 1980; 151:418–428. [PubMed: 6985950]
34. Sawahata T, Neal RA. Biotransformation of phenol to hydroquinone and catechol by rat liver microsomes. Mol. Pharmacol. 1983; 23:453–460. [PubMed: 6835203]
35. Parke DV, Williams RT. Studies in detoxication. 54. The metabolism of benzene. (a) The formation of phenylglucuronide and phenylsulphuric acid from [14C]benzene. (b) The metabolism of [14C]phenol. Biochem. J. 1953; 55:337–340. [PubMed: 13093687]
36. Smith AA. Origin of urinary pyrocatechol. Nature. 1961; 190:167. [PubMed: 13690557]
37. Bäckhed F, Ley RE, Sonnenburg JL, Peterson DA, Gordon JI. Host-bacterial mutualism in the human intestine. Science. 2005; 307:1915–1920. [PubMed: 15790844]
38. Marrubini G, et al. Direct Analysis of phenol, catechol and hydroquinone in uuman urine by coupled-column HPLC with fluorimetric detection. Chromatographia. 2005; 62:25–31.
39. Qu Q, et al. Validation of biomarkers in humans exposed to benzene: urine metabolites. Am. J. Ind. Med. 2000; 37:522–531. [PubMed: 10723046]
40. Zager RA. Combined mannitol and deferoxamine therapy for myohemoglobinuric renal injury and oxidant tubular stress. Mechanistic and therapeutic implications. J. Clin. Invest. 1992; 90:711–719. [PubMed: 1325995]
41. Paller MS, Hedlund BE. Role of iron in postischemic renal injury in the rat. Kidney Int. 1988; 34:474–480. [PubMed: 3143849]
42. Baliga R, Ueda N, Shah SV. Increase in bleomycin-detectable iron in ischaemia/reperfusion injury to rat kidneys. Biochem. J. 1993; 291:901–905. [PubMed: 7683877]
43. Jones RL, et al. Effects of iron chelators and iron overload on Salmonella infection. Nature. 1977; 267:63–65. [PubMed: 323727]
44. Freestone PP, Walton NJ, Haigh RD, Lyte M. Influence of dietary catechols on the growth of enteropathogenic bacteria. Int J Food Microbiol. 2007; 119:159–169. [PubMed: 17850907]

45. Anderson MT, Armstrong SK. Norepinephrine mediates acquisition of transferrin-iron in Bordetella bronchiseptica. J Bacteriol. 2008; 190:3940–3947. [PubMed: 18390651]
46. Richardson DR. 24p3 and its receptor: dawn of a new iron age? Cell. 2005; 123:1175–1177. [PubMed: 16377555]
47. Frisch, MJT., et al. Gaussian 03, Revision C.02. Wallingford CT: Gaussian, Inc.; 2004.
48. Kuzmic P. Program DYNAFIT for the analysis of enzyme kinetic data: application to HIV proteinase. Anal. Biochem. 1996; 237:260–273. [PubMed: 8660575]

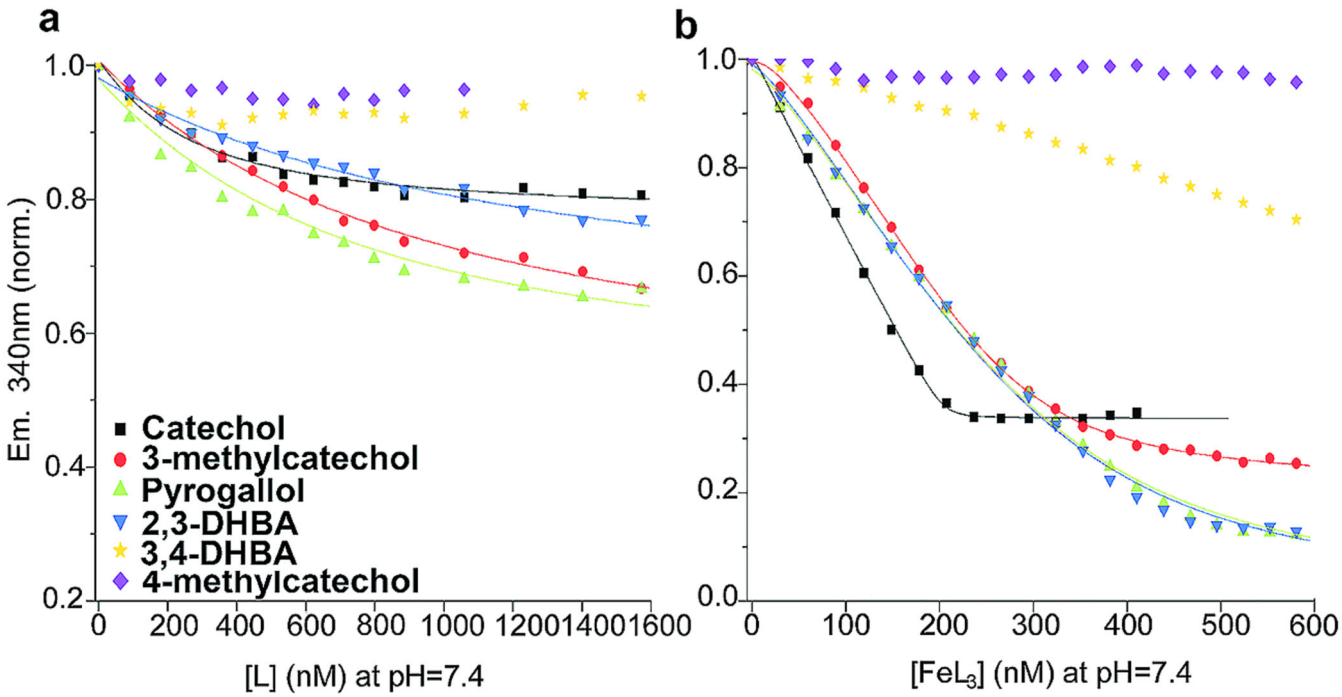

c

Ligands	Dissociation Constants L (μM)	FeL_3 K_{d1} (nM)	FeL_3 K_{d2} (nM)
Catechol	0.20±0.06	2.1±0.5	0.4±0.2
3-methylcatechol	0.9±0.1	93±2	15.6± 0.5
4-methylcatechol	>1.5	>600	-
Pyrogallol	0.8±0.3	239±15	45±3
2,3-DHBA	1.2±0.4	270±6	44±1
3,4-DHBA	>1.5	>600	-

Figure 1.

Determination of the affinity of catechol:iron in complex with Scn-Ngal. (**a**) Fluorescence quenching analysis of Scn-Ngal with free catechol ligands (L; Top) (**b**) or with $iron^{III}$ catechol ligands (FeL_3, Bottom). Symbols show the fluorescence output at 340 nm; lines are fitted using a model constructed with two dissociation constants. Note that $iron^{III}$ dramatically enhanced the affinity of Scn-Ngal for different catechols. (**c**). Calculated binding constants for free catechol (L) and $iron^{III}$ catechol (FeL_3) ligands.

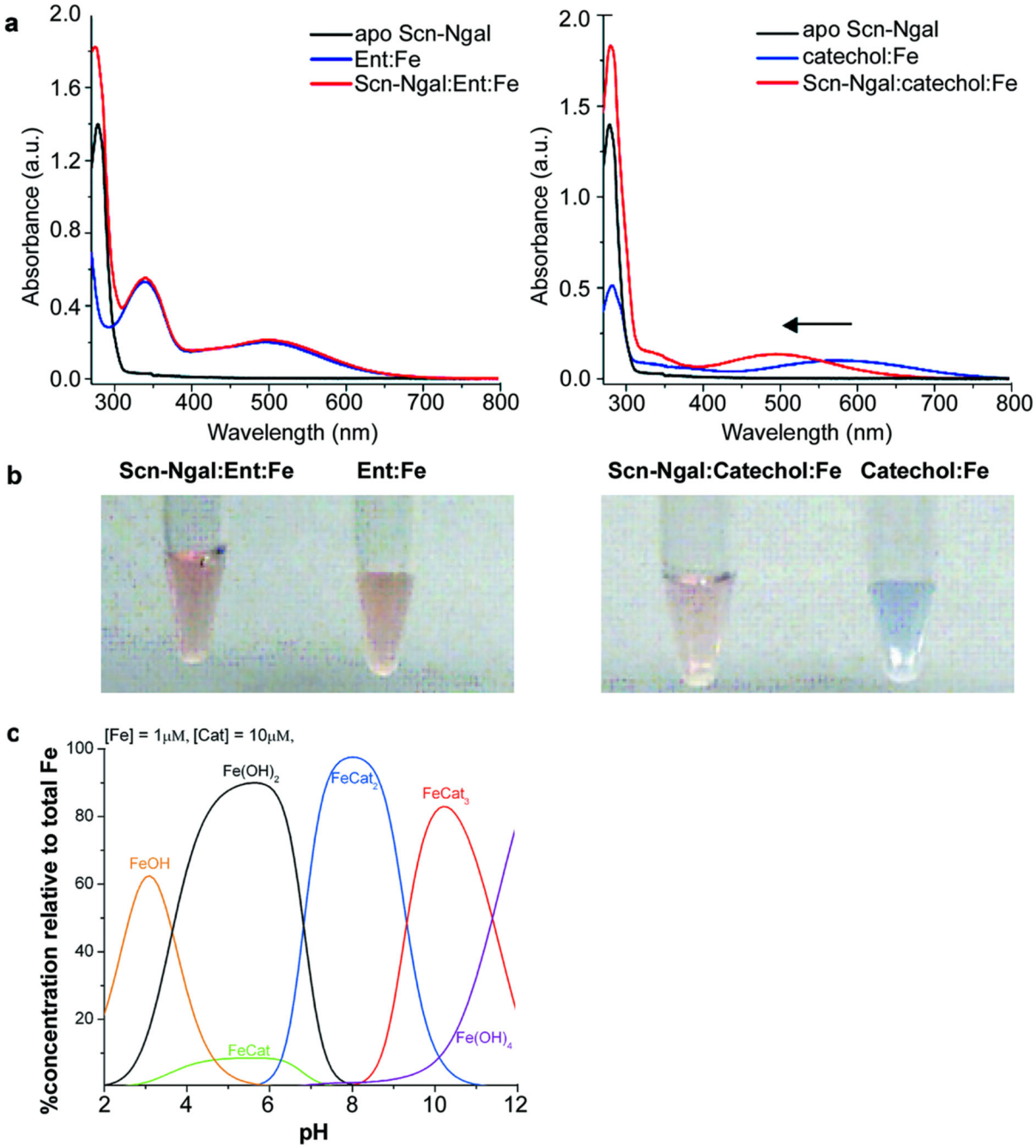

Figure 2.

UV-visible spectra of complexes of Scn-Ngal, siderophores, and iron. (**a**) apo-Scn-Ngal, Ent:iron^{III} and Scn-Ngal:Ent:iron^{III} (left) and apo-Scn-Ngal, catechol:iron^{III}, and Scn-Ngal:catechol:iron^{III} (right). While ligand-metal charge-transfers between Ent and ironIII (λ_{max} = 498 nm) were not modified by the addition of Scn-Ngal protein (note red coloration in B, 2 left tubes), catechol:iron^{III} converted from a FeL complex (blue, λ_{max} = 575 nm) to a FeL_3 complex (red, λ_{max} = 498 nm) when bound to Scn-Ngal (**b**, right tubes). (**c**) Speciation diagram of catechol:iron^{III} (10:1) in solution. FeL_2 was the predominant species at pH 7.4.

FeL_3 may be observed in more basic conditions. The speciation diagram was calculated in HySS (Hyperquad Simulation and Speciation) based on catechol thermodynamic values.

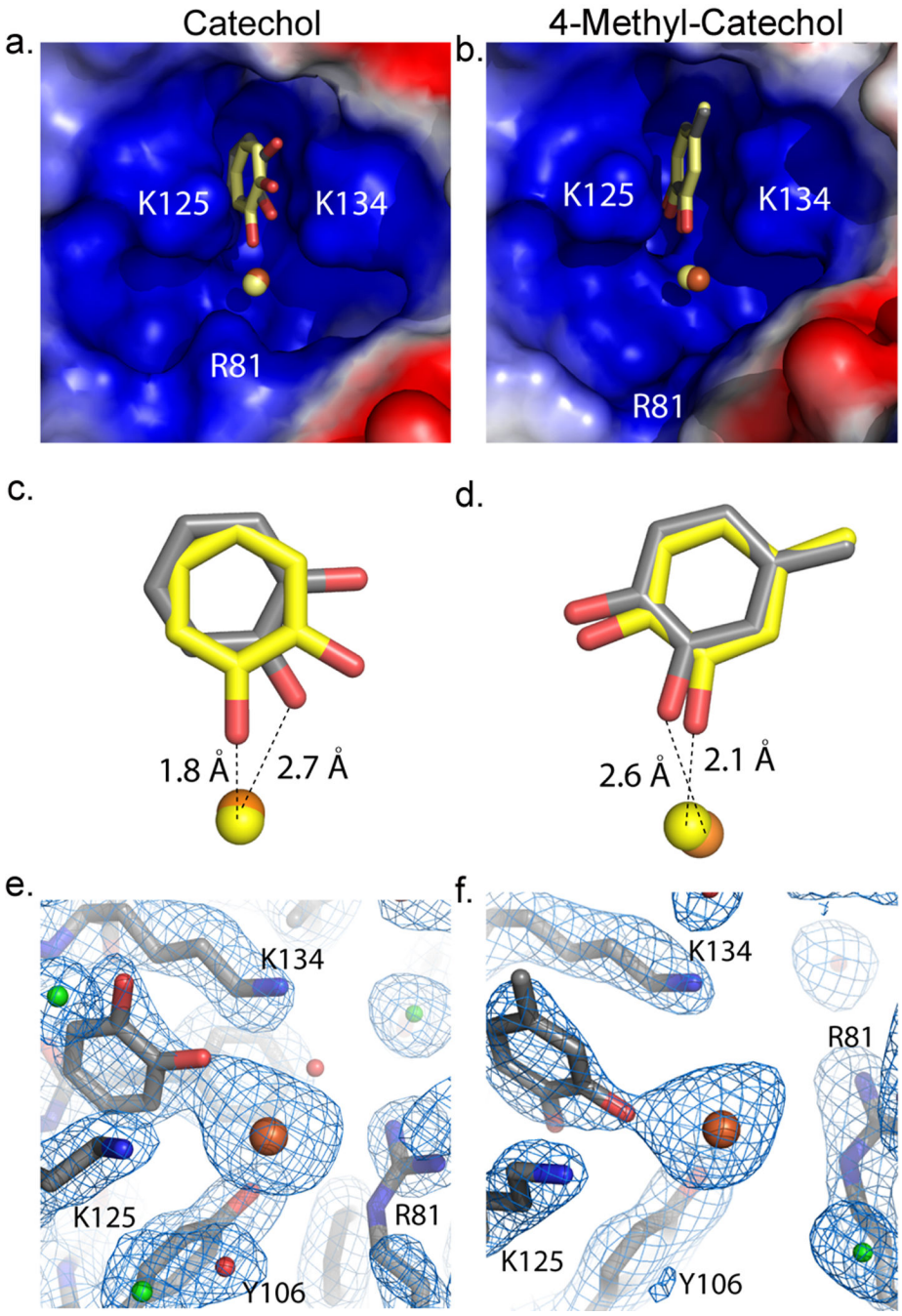

Figure 3.

Scn-Ngal binds to catechol:iron^{III} as well as to 4-methylcatechol:iron^{III}. (**a**, **b**) The images show close up views of the electrostatic surface of pocket#1 within the calyx of the protein. Positive (blue), neutral (white) and negative (red) charges are shown. Pair-wise alignment on all Cα's were used to compare the structures. The ligand in molecule A (gray) and in molecule C (yellow) are bound in pocket #1 of the calyx. (**c,d**) These panels show a side view of each ligand comparing molecule A (grey) and molecule C (yellow). Catechol (**c**) has rotated 55° towards the outside of the protein. 4-methylcatechol (**d**) has rotated 10°.

Hydroxyls groups facing out of the calyx are potentially protonated or oxidized to form a semi-quinone species. Iron is shown in orange for molecule A and yellow for molecule C in panels a–d. (**e**, **f**) 2Fo-Fc electron density map of molecule A for catechol (**e**) and 4-methylcatechol (**f**) contoured at 1 sigma. Waters are shown in red, chloride in green, iron in orange, and the molecule in gray.

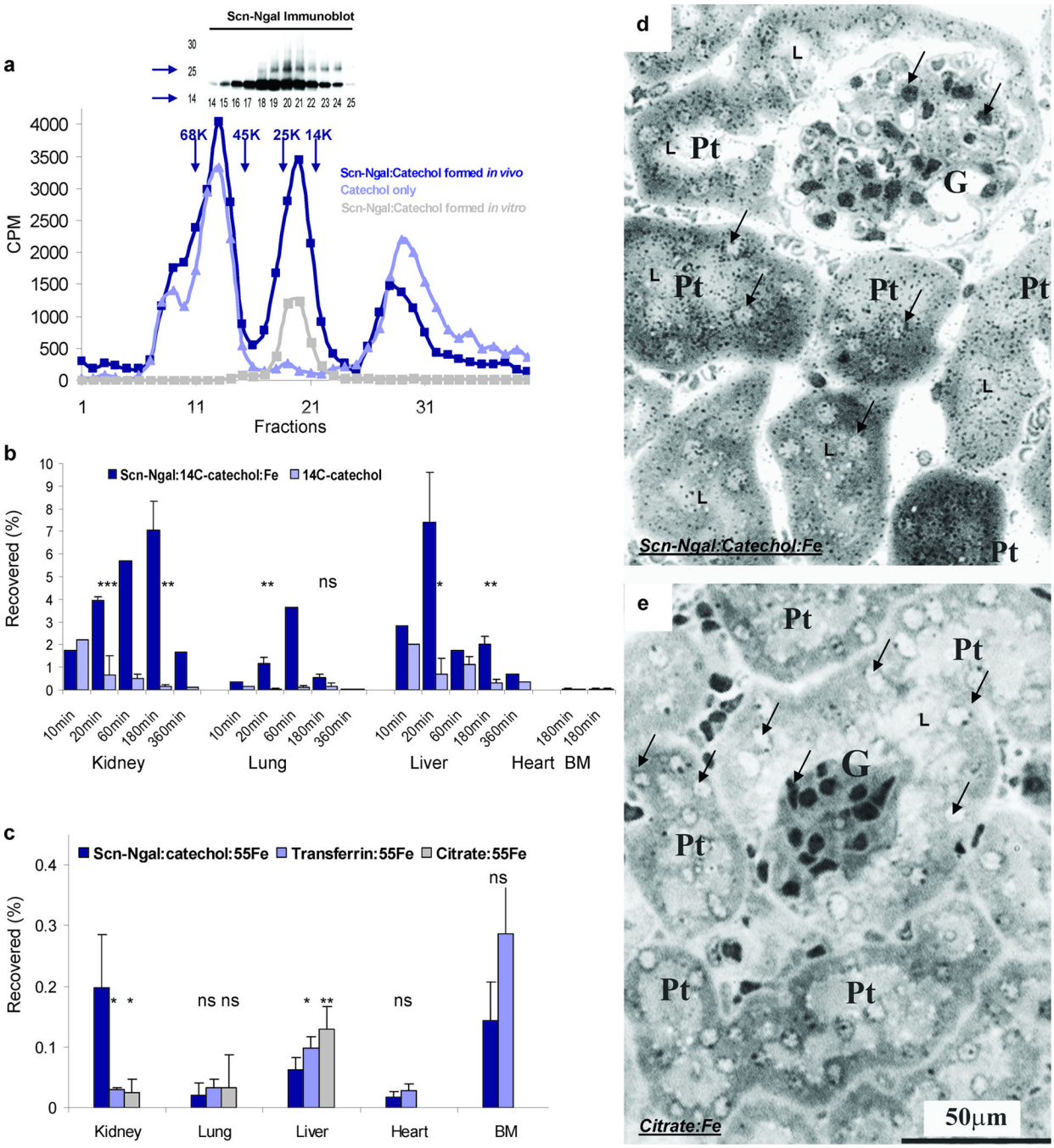

Figure 4.

The formation and distribution of the Scn-Ngal:catechol:Fe complex *in vivo*. (**a**) The Scn-Ngal:catechol complex can form in serum and be detected five minutes after i.p. injection of each component. The complex was identified by gel filtration of serum followed by immunoblots and scintillation counting (dark blue line), which revealed Ngal:^{14}C-catechol:Fe centered at fraction 20 (n = 3 independent fractionations). Also shown is the authentic Scn-Ngal:^{14}C-catechol:Fe complex formed *in vitro* (grey line) and serum taken after the injection of free ^{14}C-catechol (light blue line). (**b**) The distribution of the Scn-

Ngal:^{14}C-catechol:Fe complex vs free ^{14}C-catechol was reported as a percentage of the injected ^{14}C-catechol (n = 4 independent experiments; data represent mean ± s.d.). At 20 and 180 min, ns signifies non-significant differences, *$P < 0.05$; **$P < 0.005$; ***$P < 10^{-4}$ as assessed by two tailed Students *t*-test. (**c**) The complexes, Scn-Ngal:catechol:^{55}Fe, citrate:^{55}Fe, and transferrin:^{55}Fe were recovered at 3 hrs. Whereas Scn-Ngal:catechol:^{55}Fe located predominately to the kidney, citrate:^{55}Fe and transferrin:^{55}Fe located predominantly to the liver or bone marrow (n = 5–7 independent experiments, data represent mean ± s.d., *$P < 0.05$; **$P < 0.005$). (**d**, **e**) Trafficking of ^{55}Fe to the kidney was visualized by radioautography using Ilford K5D emulsion. Note the black silver grains in proximal tubules (Pt) after introduction of (**d**) Scn-Ngal:catechol:^{55}Fe but not after the introduction of (**e**) citrate:^{55}Fe. Glomeruli (G), proximal tubules (Pt), examples of nuclei (arrows) and tubular lumen (L) are indicated (n = 2 independent experiments).

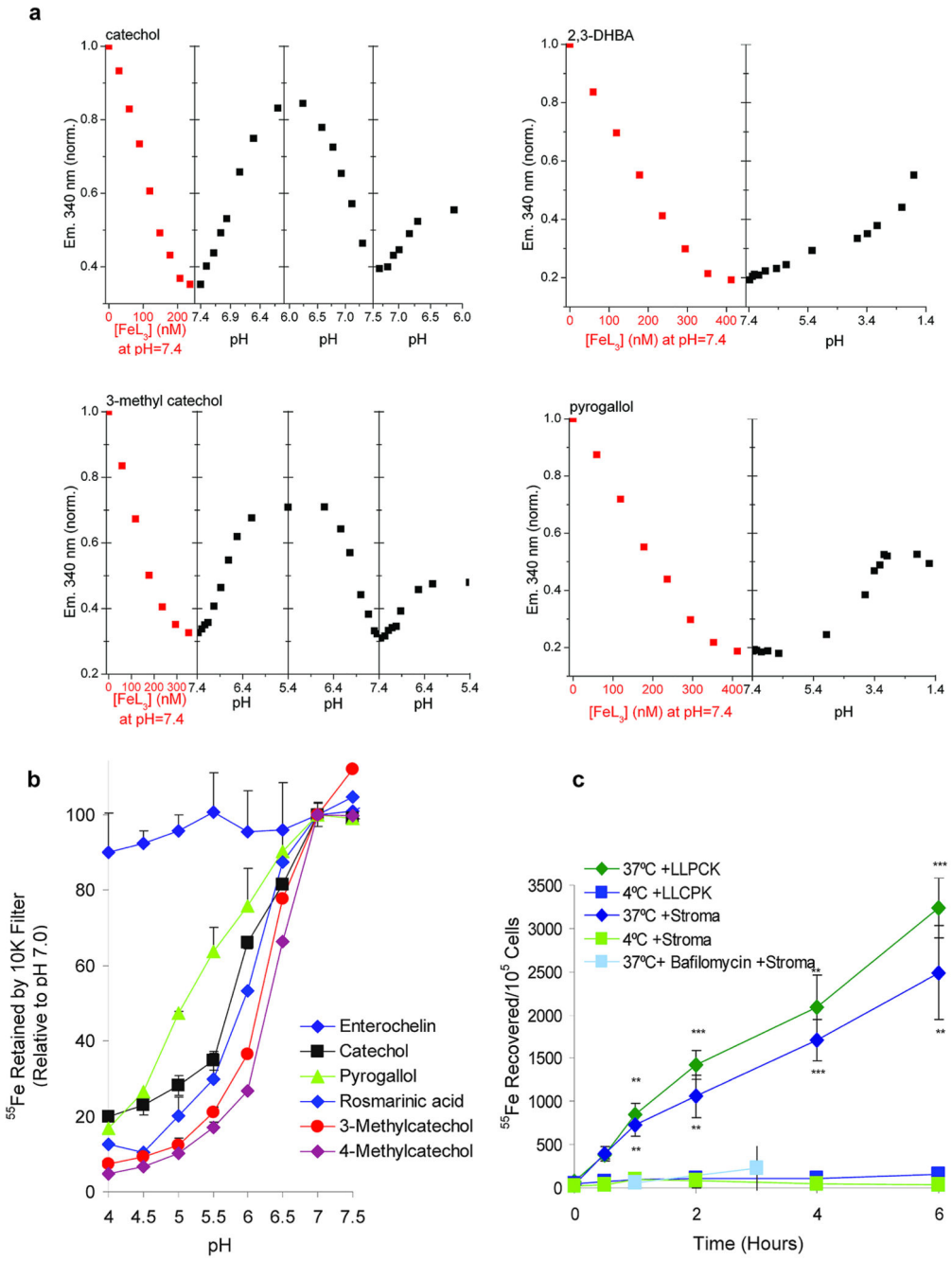

Figure 5.

Release of ligands from Scn-Ngal as a result of acidification. (**a**) Fluorescence titration of Scn-Ngal by catechol:Fe^{III}, 2,3 DHBA:Fe^{III}, 3-methycatechol:Fe^{III} and pyrogallol:Fe^{III}. Subsequently, upon acidification, the ligands were released and fluorescence returned to baseline. Basification, where relevant, caused rebinding. Note that Scn-Ngal:pyrogallol and 2,3 DHBA complexes required lower pH for dissociation. (**b**) Low pH released ^{55}Fe from Scn-Ngal:catecholate:Fe^{III} complexes. In this comparison, iron^{III} loading at pH 7.0 was defined as 100% of the assay. Catechol differed significantly from Ent (P = 0.00012) and

pyrogallol ($P = 0.0017$) at pH 5.5 (n = 4 independent preparations of Scn-Ngal, data represents mean ± s.d., two tailed *t*-test). (**c**) The capture of ^{55}Fe from the Scn-Ngal:catechol:^{55}Fe complex by kidney stromal cells and kidney proximal tubule LLCPK cells *in vitro*. ^{55}Fe uptake was inhibited at 4°C or by bafilomycin, an inhibitor of the vacuolar H^+ATPase. Data represent mean ± s.d., n =5 independent preparations of Scn-Ngal, and statistical significance (**$P < 0.005$; ***$P < 10^{-4}$) was assessed by two tailed Students *t*-test comparing uptake at 37°C and 4°C.